



## Comparison between Window Technique and Modified Stokes' Kernel in Geoid Determination for Austria

Hussein A. Abd-Elmotaal, Minia, Egypt, Norbert Kührtreiber, Graz

### Abstract

It has already been proved that there is a problem in combining the different wavelengths of the gravity field in the geoid determination process. Different approaches for correctly combining the gravity field wavelengths exist. The window technique has been suggested to get rid of the double consideration of the topographic-isostatic masses within the data window in the framework of the remove-restore technique. The modified Stokes' kernel has been suggested to possibly combine the local data signals with the global geopotential models. Both techniques have been used in computing a gravimetric geoid for Austria. The available data for the current research are described. The EGM96 geopotential model has been used. A wide comparison among classical Stokes' kernel, modified Stokes' kernel and window techniques has been carried out within this investigation in the framework of the geoid determination. The obtained results have proved that the reduced gravity anomalies using the window technique are the smoothest, un-biased and have the smallest range. Both the modified Stokes kernel and the window technique can correctly handle the combination of the geoid wavelengths within the remove-restore scheme.

**Keywords:** Stokes modified kernel, window technique, remove-restore technique, geoid determination.

### Kurzfassung

Eine bekannte Aufgabe im Rahmen der Geoidbestimmung ist die notwendige Kombination der verschiedenen Wellenlängen des Schwerfeldes der Erde. Zur korrekten Kombination existieren verschiedene Ansätze. Die „window technique“ ist eine Methode, die die doppelte Berücksichtigung der topographisch-isostatischen Massen innerhalb des Datenfensters umgeht und auf der Remove-Restore-Technik aufbaut. Eine andere mögliche Methode stellt die Modifizierung des Stokes-Kerns dar, welche die spektralen Komponenten der lokalen Daten mit den Signalen eines globalen Erdschwermodells kombiniert. Beide Methoden werden zur Berechnung eines gravimetrischen Geoids von Österreich verwendet. Die zur Untersuchung verwendeten Daten werden eingehend beschrieben. Als globales Erdschwermodell wird EGM96 verwendet. Ein ausführlicher Vergleich zwischen den verschiedenen Methoden, der klassischen Geoidberechnung mittels Stokes, der „window technique“ und der Methode des modifizierten Stokes-Kerns wird auf Basis der Geoidhöhe durchgeführt. Die homogensten Schwereanomalien (trendfrei, kleinste Extremwerte) werden durch die Anwendung der „window technique“ zur Schwereerdrückung erreicht. Die Ergebnisse zeigen, dass mittels beider Methoden eine korrekte Kombination der unterschiedlichen Wellenlängen des Geoids möglich ist.

**Schlüsselwörter:** Modifizierung des Stokes-Kerns, „window technique“, Remove-Restore-Technik, Geoidberechnung

### 1. Introduction

The optimum combination of the different wavelengths of the gravity field is a critical research point. There are different approaches for such a combination of wavelengths. The current investigation considers a comparison of two approaches, namely the window technique (Abd-Elmotaal and Kührtreiber, 2003) [1] and the modified Stokes' kernel technique.

The used data sets are described. The Stokes' technique of geoid determination, within the remove-restore scheme, with classical un-modified and modified Stokes' kernel, after Meissl (1971) [7], is described. The window technique (Abd-Elmotaal and Kührtreiber, 2003) [1] within the remove-restore scheme has been outlined. The harmonic analysis of the topographic-isostatic

potential is then given. The reduced gravity using both techniques under investigations are then computed and compared. Both techniques, as well as the traditional Stokes' kernel, have been used in computing a gravimetric geoid for Austria. A wide comparison among classical Stokes' kernel, modified Stokes' kernel and window techniques has been carried out within this investigation in the framework of the geoid determination. The comparison is made on two different levels: the residual gravity anomalies after the remove step and the computed geoid signals.

It should be noted that many scholars have suggested different modifications of the Stokes' kernel and have studied the topic of the optimum combination of gravity field wavelengths. The reader may refer, e.g., to Sjöberg and Hunegnaw

(2000) [14]; Novák et al. (2001) [8]; Sjöberg (2003a) [11]; (2003b) [12]; (2004) [13]; Vaníček and Featherstone (1998) [16]; Featherstone (1999) [2]; (2003) [3]; Huang et al. (2000) [6]; Silva et al. (2002) [10].

## 2. The Used Data

### 2.1 Gravity Data

The gravitational data set for this investigation is a set of free-air gravity anomalies at 5796 stations in Austria and neighbouring countries (Fig. 1). Fig. 1 shows, more or less, a homogeneous data distribution within Austria. The gravity data outside Austria have been included to correct the edge effect in the computed gravimetric geoid for Austria. The gravity data covers the window  $(45.7^\circ\text{N} \leq \phi \leq 49.7^\circ\text{N}$  and  $8.5^\circ\text{E} \leq \lambda \leq 18.2^\circ\text{E}$ ).

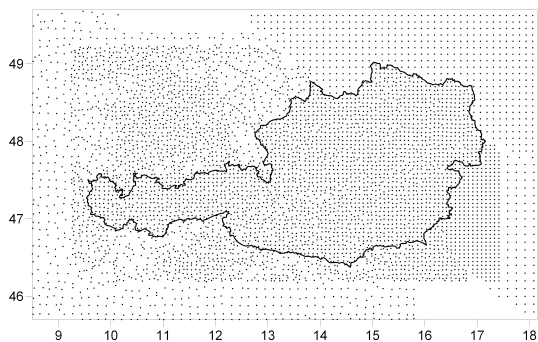


Fig. 1: Distribution of the used gravity data set

### 2.2 GPS Benchmarks

Fig. 2 shows the distribution of the available GPS (referred to ITRF96) benchmarks with known orthometric heights (referred to UELN98) in Austria. It shows that most of the stations are located in the eastern part of Austria. Only few stations are located at the mountainous western part of Austria.

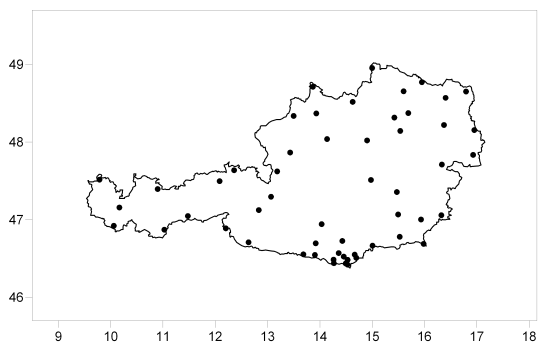


Fig. 2: Used GPS benchmarks with known orthometric heights

### 2.3 Digital Height Models

Two different digital height models are available. A coarse model of  $90'' \times 150''$  resolution in the latitude and the longitude directions, respectively, and a fine model of  $11.25'' \times 18.75''$  resolution. The fine DHM covers the window  $44.75^\circ\text{N} \leq \phi \leq 50.25^\circ\text{N}$ ;  $7.75^\circ\text{E} \leq \lambda \leq 19.25^\circ\text{E}$ . The coarse DHM covers the window  $40^\circ\text{N} \leq \phi \leq 52^\circ\text{N}$ ;  $5^\circ\text{E} \leq \lambda \leq 22^\circ\text{E}$ .

The coarse DHM has been created by integrating the Austrian fine DHM with GTOPO30 ( $30'' \times 30''$ ) (Gesch and Larson, 1996) [4] and global bathymetry model provided by the Naval Oceanographic Office ( $1' \times 1'$ ). Fig. 3 shows the coarse digital height model used for this investigation. It shows the high mountainous structure of the Alps.

### 3. Traditional Remove-Restore Technique

Within the well-known remove-restore technique, the effect of the topographic-isostatic masses is removed from the source gravitational data and then restored to the resulting geoidal heights. For example, in the case of gravity data, the reduced gravity anomalies in the framework of the remove-restore technique is computed by

$$\Delta g_{red} = \Delta g_F - \Delta g_{GM} - \Delta g_h, \quad (1)$$

where  $\Delta g_F$  stands for the free-air anomalies,  $\Delta g_h$  is the effect of topography and its compensation on the gravity anomalies, and  $\Delta g_{GM}$  is the effect of the reference field on the gravity anomalies. Thus the final computed geoid  $N$  within the remove-restore technique can be expressed by:

$$N = N_{GM} + N_{\Delta g} + N_h, \quad (2)$$

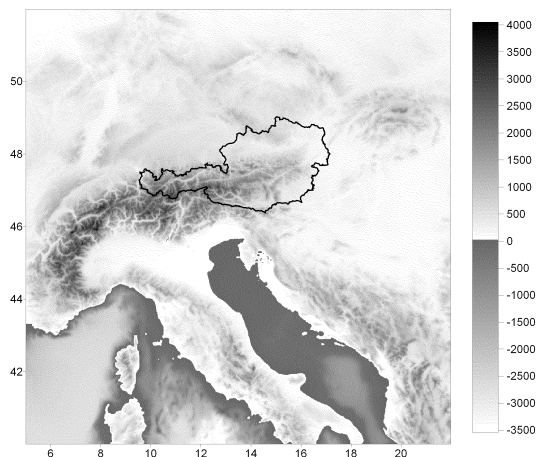


Fig. 3: The coarse ( $90'' \times 150''$ ) digital height model

where  $N_{GM}$  gives the contribution of the reference field,  $N_{\Delta g}$  gives the contribution of the reduced gravity anomalies, and  $N_h$  gives the contribution of the topography and its compensation (the indirect effect).

**4. Stokes' Integral with Classical Stokes' Kernel**

The contribution of the reduced gravity anomalies  $N_{\Delta g}$  can be given by Stokes' integral (Heiskanen and Moritz, 1967, p. 94) [5]

$$N_{\Delta g} = \frac{R}{4\pi\gamma} \int \int \Delta g_{red} S(\psi) d\sigma, \tag{3}$$

where  $\gamma$  is the normal gravity,  $R$  is the mean earth's radius and  $S(\psi)$  stands for the classical Stokes' kernel given by (ibid., p. 94) [5]

$$S(\psi) = \frac{1}{s} - 4 - 6s + 10s^2 - (3 - 6s^2) \ln(s + s^2), \tag{4}$$

with

$$s = \sin \frac{\psi}{2}, \tag{5}$$

and  $\psi$  is the spherical distance between the computational point  $P$  and the running point  $Q$ .

It is believed that using classical un-modified Stokes kernel in the remove-restore technique implies a wrong combination of gravity field wavelengths. This will be proved in the sequel.

**5. Stokes' Integral with Modified Stokes' Kernel**

The contribution of the reduced gravity anomalies  $N_{\Delta g}$  can be given by

$$N_{\Delta g} = \frac{R}{4\pi\gamma} \int \int \Delta g_{red} S^{ME}(\psi) d\sigma, \tag{6}$$

where  $S^{ME}(\psi)$  is the modified Stokes' kernel after Meissl (1971) [7] given by

$$S^{ME}(\psi) = S(\psi) - S(\psi_o) \text{ for } (0 < \psi < \psi_o), \tag{7}$$

where the optimal cap size  $\psi_o$  is empirically determined through the comparison to the GPS/levelling derived geoid.

**6. The Window Technique**

The conventional way of removing the effect of the topographic-isostatic masses faces a theoretical problem. A part of the influence of the topographic-isostatic masses is removed twice as it is already included in the global reference field. This leads to some double consideration of that part of the topographic-isostatic masses. Fig. 4 shows schematically the conventional gravity reduction for the effect of the topographic-isostatic masses. The short-wavelength part depending on the

topographic-isostatic masses is computed for a point  $P$  for the masses inside the circle (say till 167 km around the computational point  $P$ ). Removing the effect of the long-wavelength part by a global earth's gravitational potential reference field normally implies removing the influence of the global topographic-isostatic masses, shown as a rectangle in Fig. 4. The double consideration of the topographic-isostatic masses inside the circle (double hatched) is thus seen.

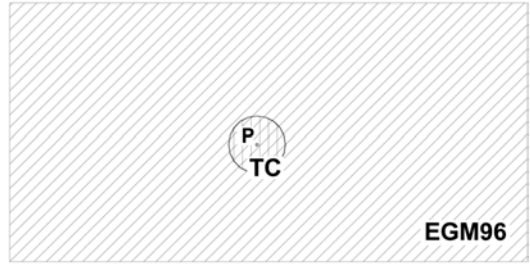


Fig. 4: The traditional remove-restore technique

A possible way to overcome this difficulty is to adapt the used reference field due to the effect of the topographic-isostatic masses for a fixed data window. Fig. 5 shows the advantage of the window remove-restore technique schematically. Consider a measurement at point  $P$ , the short-wavelength part depending on the topographic-isostatic masses is now computed by using the masses of the whole data area (small rectangle). The adapted reference field is created by subtracting the effect of the topographic-isostatic masses of the data window, in terms of potential coefficients, from the reference field coefficients. Thus, removing the long-wavelength part by using this adapted reference field does not lead to a double consideration of a part of the topographic-isostatic masses (no double hatched area in Fig. 5).

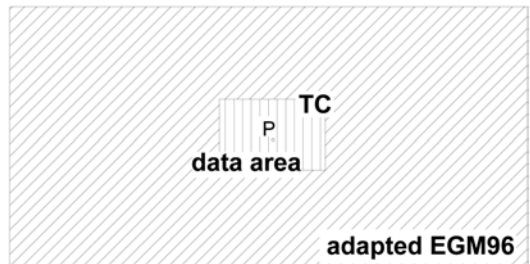


Fig. 5: The window remove-restore technique

The remove step of the window remove-restore technique can then mathematically be written as

$$\Delta g_{red} = \Delta g_F - \Delta g_{GM\ Adapt} - \Delta g_h, \quad (8)$$

where  $\Delta g_{GM\ Adapt}$  is the contribution of the adapted reference field. The restore step of the window remove-restore technique can be written as

$$N = N_{GM\ Adapt} + N_{\Delta g} + N_h, \quad (9)$$

where  $N_{GM\ Adapt}$  gives the contribution of the adapted reference field.

It should be noted that the contribution of the reduced gravity anomalies  $N_{\Delta g}$  is computed using the Stokes' integral (3) with the classical unmodified Stokes' kernel given by (4).

## 7. Harmonic Analysis of the Topographic-Isostatic Potential

The harmonic coefficients of the topography and its isostatic compensation as well as the harmonic series expansion of the topographic-isostatic potential can be expressed by (Abd-Elmotaal and Kührtreiber, 2003, pp. 78–79) [1]:

$$T_{TI}(P) = \frac{GM}{r_p} \sum_{n=0}^{\infty} \left(\frac{R}{r_p}\right)^n \sum_{m=-n}^n \bar{T}_{nm} \bar{R}_{nm}(P), \quad (10)$$

where

$$\begin{aligned} \bar{T}_{nm} = & \frac{R^3}{M(2n+1)(n+3)} \iint_{\sigma} \left\{ \delta\rho_Q \left[ \left(1 + \frac{H_Q}{R}\right)^{n+3} - 1 \right] + \right. \\ & \left. + \delta\rho_Q \left(1 - \frac{T_o}{R}\right)^{n+3} \left[ \left(1 - \frac{t_Q}{R-T_o}\right)^{n+3} - 1 \right] \right\} \bar{R}_{nm}(Q) d\sigma_Q \end{aligned} \quad (11)$$

where  $T_o$  is the normal crustal thickness,  $H$  is the topographic height,  $t$  is the compensating root/antiroot and  $M$  denotes the mass of the earth, given by

$$M \cong \frac{4\pi R^3}{3} \rho_M, \quad (12)$$

where  $\rho_M$  denotes the mean earth's density (Sünkel, 1985) [15]

$$\rho_M \cong 5.517 \text{ g/cm}^3.$$

For the practical determination of the harmonic coefficients of the topographic-isostatic potential, (11) may be written as

$$\begin{aligned} \bar{T}_{nm} = & \frac{3\Delta\phi\Delta\lambda}{4\pi\rho_M(2n+1)(n+3)} \sum_i^{\phi} \sum_j^{\lambda} \left\{ \rho_{ij} \left[ \left(1 + \frac{H_{ij}}{R}\right)^{n+3} - 1 \right] + \right. \\ & \left. + \Delta\rho_{ij} \left(1 - \frac{T_o}{R}\right)^{n+3} \left[ \left(1 - \frac{t_{ij}}{R-T_o}\right)^{n+3} - 1 \right] \right\} \\ & \cdot \left\{ \begin{array}{l} \cos m\lambda_j \\ \sin m\lambda_j \end{array} \right\} \bar{P}_{nm}(\cos\theta_i) \cos\theta_i, \end{aligned} \quad (13)$$

where  $\sum$  denotes the summation along  $\phi$  and  $\lambda$ ,  $\Delta\phi$  and  $\Delta\lambda$  are the grid sizes of the used digital

height model in the latitude and the longitude directions, respectively,  $\rho$  is given by

$$\begin{aligned} \rho &= \rho_o & \text{for } H \geq 0, \\ \rho &= \rho_o - \rho_w & \text{for } H < 0, \end{aligned} \quad (14)$$

where  $\rho_o$  denotes the density of the topography and  $\rho_w$  is the density of ocean's water. The density anomaly  $\Delta\rho$  is given by

$$\Delta\rho = \rho_1 - \rho_o, \quad (15)$$

where  $\rho_1$  is the density of the upper mantle.

In case of the Airy-Heiskanen isostatic model, the thickness of the root/antiroot  $t$  is determined by applying the principle of mass balance, which can be written in the spherical approximation as (Rummel et al., 1988, p. 3) [9]

$$\begin{aligned} \rho_o R^3 \left[ \left(1 + \frac{H}{R}\right)^3 - 1 \right] = \\ = (\rho_1 - \rho_o)(R - T_o)^3 \left[ 1 - \left(1 - \frac{t}{R-T_o}\right)^3 \right]. \end{aligned} \quad (16)$$

This condition can be written for the thickness of the root/antiroot  $t$  as follows:

$$\frac{t}{R-T_o} = 1 - \left\{ 1 - \frac{\rho}{\rho_1 - \rho_o} \left(1 - \frac{T_o}{R}\right)^{-3} \left[ \left(1 + \frac{H}{R}\right)^3 - 1 \right] \right\}^{\frac{1}{3}}, \quad (17)$$

where  $\rho$  is given by (14).

## 8. Gravity Reduction

The following parameter set has been used during the gravity reduction and the geoid determination process:

$$T_o = 30 \text{ km}, \quad (18)$$

$$\rho_o = 2.67 \text{ g/cm}^3, \quad (19)$$

$$\Delta\rho = 0.2 \text{ g/cm}^3. \quad (20)$$

The EGM96 geopotential model has been used for the traditional remove-restore technique. An adapted reference field has been created by subtracting the potential coefficients of the topographic-isostatic masses of the data window ( $40^\circ\text{N} \leq \phi \leq 52^\circ\text{N}$ ;  $5^\circ\text{E} \leq \lambda \leq 22^\circ\text{E}$ ) computed by (13) from the EGM96 coefficients. This adapted reference field has been used for the window remove-restore technique.

Table 1 shows the statistics of the gravity reduction after each reduction step for the traditional and window remove-restore techniques. It should be noted that the reduced anomalies for Stokes' integral with modified Stokes' integral are the same as those for the Stokes' integral with the classical unmodified Stokes' integral (the upper part of the table).

Reduced gravity	Statistical parameters (mgal)			
	Min.	Max.	Average	St. dev.
$\Delta g_F$	-154.16	187.15	9.70	42.16
$\Delta g_F - \Delta g_{GM}$	-210.72	132.27	-12.91	37.60
$\Delta g_F - \Delta g_{GM} - \Delta g_{TI}$	-123.66	81.97	-20.09	25.88
$\Delta g_F - \Delta g_{GM Adapt}$	-194.55	204.99	-1.46	44.43
$\Delta g_F - \Delta g_{GM Adapt} - \Delta g_{TI Win}$	-62.39	71.60	0.23	20.32

Table 1: Statistics of the reduced gravity after each reduction step

Table 1 shows that using the window technique gives the best reduced gravity anomalies. The range has dropped to its one-third and the standard deviation drops by about 20%. Also the reduced anomalies are perfectly centered (un-biased). This property makes the window-technique reduced anomalies suit best for interpolation and other geodetic purposes.

- Stokes' integral using Meissl's modified Stokes' kernel (Stokes/Meissl geoid),
- Stokes' integral using window technique (Window geoid).

All computed geoids are compared to the GPS/levelling derived geoid.

### 9. Geoid Determination for Austria

Three methods are used in the current investigation to compute a gravimetric geoid for Austria. They are:

- Stokes' integral using classical un-modified Stokes' kernel (classical Stokes geoid),

Fig. 6 shows the absolute geoid differences between the classical Stokes geoid and the GPS/levelling derived geoid. Fig. 6 shows a high-order polynomial structure of the differences. The range of the differences is quite large (about 2 m).

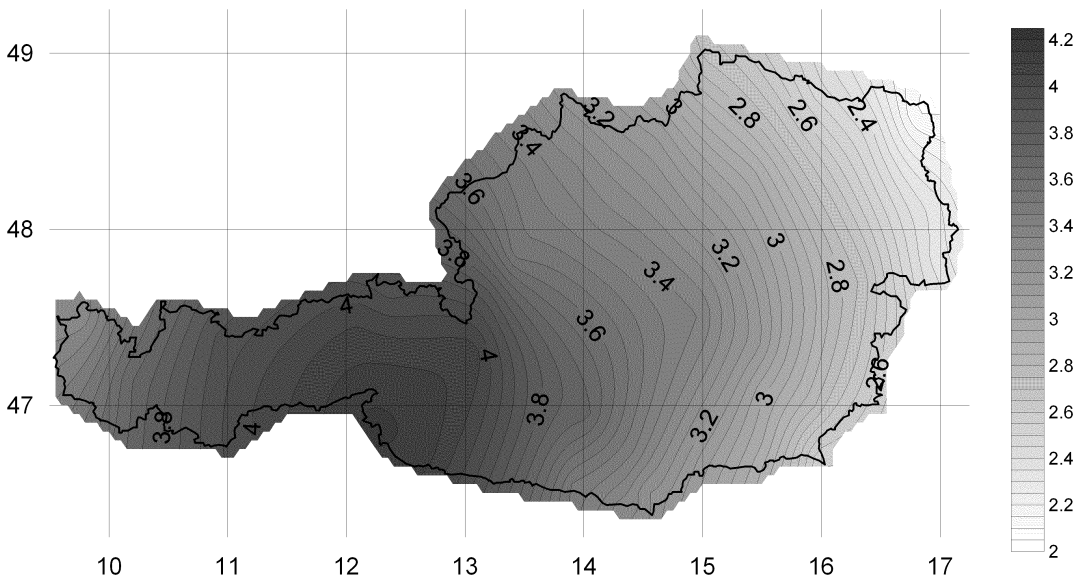


Fig. 6: Absolute geoid differences between classical Stokes geoid and GPS/levelling derived geoid. Contour interval: 5 cm

Cap size	Differences to GPS/levelling derived geoid (m)			
	Min.	Max.	Average	St. dev.
$\psi_o = 0.5^\circ$	-4.58	-1.31	-2.57	0.81
$\psi_o = 1.0^\circ$	-2.73	-1.28	-1.90	0.40
$\psi_o = 1.5^\circ$	-1.69	-1.09	-1.30	0.14
$\psi_o = 1.7^\circ$	-1.37	-0.91	-1.08	0.10
$\psi_o = 2.0^\circ$	-1.10	-0.44	-0.78	0.14

Table 2: Statistics of the empirical tests for the cap size  $\psi_o$  for the Stokes/Meissl geoid

As mentioned earlier, the optimum cap size  $\psi_o$  can be empirically determined. This is achieved by comparing the computed Stokes/Meissl geoid to the GPS/levelling derived geoid. Table 2 shows the statistics of the empirical tests for the cap size  $\psi_o$  for the Stokes/Meissl geoid. It shows that  $\psi_o = 1.7^\circ$  gives the optimum cap size in view of the standard deviation of the absolute differences to the GPS/levelling derived geoid.

Fig. 7 shows the absolute geoid differences between the Stokes/Meissl geoid (cap size

$\psi_o = 1.7^\circ$ ) and the GPS/levelling derived geoid. Fig. 7 shows a better polynomial structure of the differences than that in the case of Stokes geoid. The range of the differences drops to about 45 cm.

Fig. 8 shows the absolute geoid differences between the window geoid and the GPS/levelling derived geoid. Fig. 8 shows a better polynomial structure of the differences than that in the case of Stokes geoid. The range of the differences drops to about 1 m.

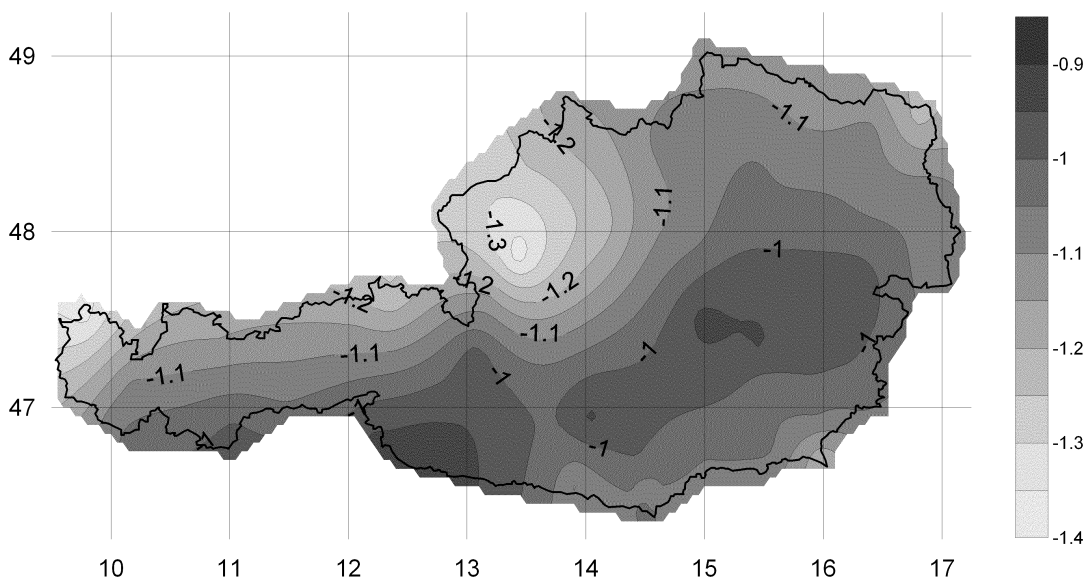


Fig. 7: Absolute geoid differences between Stokes/Meissl geoid (cap size  $\psi_o = 1.7^\circ$ ) and GPS/levelling derived geoid. Contour interval: 5 cm

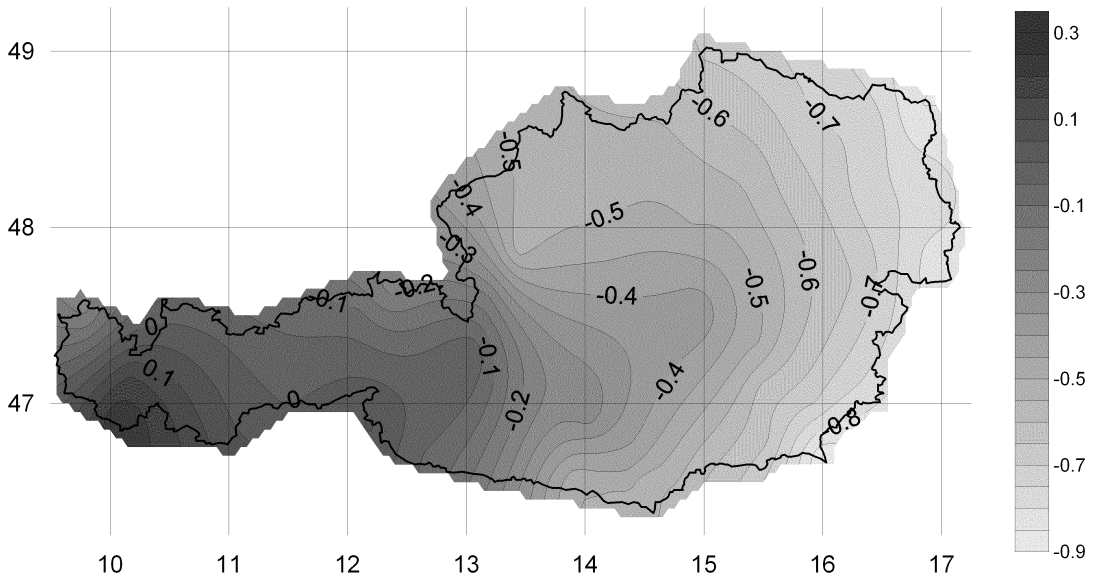


Fig. 8: Absolute geoid differences between window geoid and GPS/levelling derived geoid. Contour interval: 5 cm

Geoid technique	Statistical parameters (m)			
	Min.	Max.	Average	St. dev.
Stokes	2.10	4.16	3.27	0.52
Stokes/Meissl	-1.37	-0.91	-1.08	0.10
Window	-0.89	0.24	-0.44	0.27

Table 3: Statistics of the absolute geoid differences between the computed geoids and the GPS/levelling derived geoid

Table 3 illustrates the statistics of the absolute geoid differences between the computed geoids within the current investigation and the GPS/levelling derived geoid. Table 3 shows that the Stokes geoid has the worst differences to the GPS/levelling derived geoid. This confirms what has been stated earlier that using the classical unmodified Stokes kernel in the remove-restore technique implies a wrong combination of gravity field wavelengths. Table 3 shows also that either using the window technique or the modified

Stokes' kernel gives better differences to the GPS/levelling derived geoid (in terms of either the mean difference or the range/standard deviation).

Table 4 illustrates the statistics of the geoid differences between the computed geoids within the current investigation and the GPS/levelling derived geoid after removing a third order surface polynomial trend function. Table 4 shows that the window technique gives the minimum range and standard deviation of the remaining differences.

Geoid technique	Statistical parameters (cm)			
	Min.	Max.	Average	St. dev.
Stokes	-22.1	16.7	38.8	7.3
Stokes/Meissl	-25.3	12.5	37.8	6.9
Window	-21.3	14.8	36.1	6.6

Table 4: Statistics of the geoid differences between the computed geoids and the GPS/levelling derived geoid after removing a trend function

## 10. Conclusions

Stokes technique, within the remove-restore scheme, with the classical un-modified Stokes' kernel cannot correctly handle the combination of the geoid wavelengths. A modification of the kernel or a new technique should be introduced. Both the modified Stokes' kernel and the window technique can correctly handle the combination of the geoid wavelengths within the remove-restore scheme. The reduced gravity anomalies using the window technique are the smoothest (20% less in the standard deviation), un-biased and have the smallest range (one-third less). This property makes the window-technique reduced anomalies suit best for interpolation and other geodetic purposes.

## References

- [1] *Abd-Elmotaal, H., Kühtreiber, N. (2003):* Geoid Determination Using Adapted Reference Field, Seismic Moho Depths and Variable Density Contrast, *Journal of Geodesy*, 77, 77–85.
- [2] *Featherstone, W. (1999):* A Comparison of Gravimetric Geoid Models over Western Australia, Computed using Modified Forms of Stokes' Integral, *Journal of the Royal Society of Western Australia*, 82, 137–145.
- [3] *Featherstone, W. (2003):* Software for Computing Five Existing Types of Deterministically Modified Integration Kernel for Gravimetric Geoid Determination, *Computers* 193.
- [4] *Gesch, D.B., Larson, K.S. (1996):* Techniques for Development of Global 1-Kilometer Digital Elevation Models, In: *Pecora Thirteen, Human Interactions with the Environment – Perspectives from Space*, Sioux Falls, South Dakota, August 20–22, 1996.
- [5] *Heiskanen, W.A., Moritz, H. (1967):* *Physical Geodesy*, Freeman, San Francisco.
- [6] *Huang, J., Vaniček, P., Novák, P. (2000):* An Alternative Algorithm to FFT for the Numerical Evaluation of Stokes' Integral, *Studia geoph. et geod.*, 44, 374–380.
- [7] *Meissl, P. (1971):* A Study of Covariance Functions Related to the Earth's Disturbing Potential, Department of Geodetic Science, The Ohio State University, Columbus, Ohio, 151.
- [8] *Novák, P., Vaniček, P., Véronneau, M., Holmes, S., Featherstone, W. (2001):* On the Accuracy of the Modified Stokes' Integration in High-Frequency Gravimetric Geoid Determination, *Journal of Geodesy*, 74, 644–654.
- [9] *Rummel, R., Rapp, R.H., Sünkel, H., Tscherning, C.C. (1988):* Comparison of Global Topographic/Isostatic Models to the Earth's Observed Gravity Field, Department of Geodetic Science, The Ohio State University, Columbus, Ohio, 388.
- [10] *Silva, M.A., Blitzkow, D., Lobianco, M.C.B. (2002):* A Case Study of Different Modified Kernel Applications in Quasi-Geoid Determination, *Proceedings of the 3<sup>rd</sup> Meeting of the International Gravity and Geoid Commission*, Thessaloniki, Greece, August 26–30, 2002, 138–143.
- [11] *Sjöberg, L.E. (2003a):* A Computational Scheme to Model the Geoid by the Modified Stokes' Formula Without Gravity Reductions, *Journal of Geodesy*, 77, 423–432.
- [12] *Sjöberg, L.E. (2003b):* A General Model for Modifying Stokes' Formula and its Least-Squares Solution, *Journal of Geodesy*, 77, 459–464.
- [13] *Sjöberg, L.E. (2004):* A Spherical Harmonic Representation of the Ellipsoidal Correction to the Modified Stokes' Formula, *Journal of Geodesy*, 78, 180–186.
- [14] *Sjöberg, L.E., Hunegnaw, A. (2000):* Some Modifications of Stokes' Formula that Account for Truncation and Potential Coefficient Errors, *Journal of Geodesy*, 74, 232–238.
- [15] *Sünkel, H. (1985):* An Isostatic Earth Model, Department of Geodetic Science, The Ohio State University, Columbus, Ohio, 367.
- [16] *Vaniček, P., Featherstone, W. (1998):* Performance of Three Types of Stokes' Kernel in the Combined Solution for the Geoid, *Journal of Geodesy*, 72, 684–697.

## Contact

**Hussein A. Abd-Elmotaal**, Civil Engineering Department, Faculty of Engineering, Minia University, Minia, Egypt  
email: [abdeltmotaal@lycos.com](mailto:abdeltmotaal@lycos.com)

**Norbert Kühtreiber**, Institute of Navigation and Satellite Geodesy, TU Graz, Steyrergasse 30, A-8010 Graz, Austria  
e-mail: [norbert.kuehtreiber@tugraz.at](mailto:norbert.kuehtreiber@tugraz.at)